

# Predicting laser-induced cavitation near a solid substrate

Fabian Denner<sup>1,\*</sup>, Fabien Evrard<sup>1</sup>, Fabian Reuter<sup>2</sup>, Silvestre Roberto Gonzalez-Avila<sup>3</sup>, Berend van Wachem<sup>1</sup>, and Claus-Dieter Ohl<sup>2</sup>

<sup>1</sup> Chair of Mechanical Process Engineering, Institute of Process Engineering, Otto-von-Guericke-Universität Magdeburg, Universitätsplatz 2, 39106 Magdeburg, Germany

<sup>2</sup> Department Soft Matter, Institute of Physics, Otto-von-Guericke-Universität Magdeburg, Universitätsplatz 2, 39106 Magdeburg, Germany

<sup>3</sup> University of Poitiers – École Nationale Supérieure de Mécanique et d'Aérotechnique (ENSMA) Téléport 2, 1 Avenue Clément Ader, 86360 Chasseneuil-du-Poitou, France.

The asymmetric collapse of cavitation bubbles near a solid substrate generates large wall shear stresses, the precise magnitude of which is still not known with certainty. By comparing numerical simulations and experiments of a laser-induced cavitation bubble near a solid substrate, we demonstrate that an accurate measurement of the pressure pulse emitted during bubble inception and of the maximum bubble radius allow a unique initialisation of the simulation. This allows an accurate reproduction of the asymmetric collapse, with reliable predictions of the shear stress and pressure generated at the substrate.

© 2021 The Authors *Proceedings in Applied Mathematics & Mechanics* published by Wiley-VCH GmbH

## 1 Introduction

A cavitation bubble near a solid substrate collapses asymmetrically and produces a fast liquid jet, which in turn generates large shear stresses on the substrate that can exceed 100 kPa [1]. Such jetting cavitation bubbles may cause detrimental material erosion but are also utilised successfully, for instance, in laser ablation technologies and in ultrasonic cleaning. Laser-induced cavitation offers a reproducible and controllable means of generating such cavitation bubbles individually in predefined locations, through optical breakdown of the liquid and the subsequent formation of a gas cavity. While experiments and Rayleigh-Plesset models have provided a very good understanding of the related bubble dynamics, especially the shear stresses generated on the substrate and nearby objects are still not known in detail. To this end, accurate numerical simulations can provide valuable insight, however, previous experiments [2] and numerical simulations [1] produced contradictory results. Typically, the maximum radius of the cavitation bubble is the only reference value used in simulations when reproducing a given experiment [1, 3]. In this article, we show that a measurement of the pressure pulse emitted during bubble inception together with the maximum bubble radius provide a unique set of reference values to guide the selection of the initial conditions for accurate and reliable simulations of the asymmetric collapse of laser-induced cavitation bubbles.

## 2 Methods

In the experiments, the cavitation bubble is created inside the test section at a distance  $h_0$  above the substrate by a focused laser beam using a Q-switched Nd:YAG laser (New Wave Research, wavelength 532 nm, pulse duration 6 ns, laser beam diameter 2.75 mm), as described in more detail in [4]. Fig. 1a shows high-speed images of the considered bubble, with maximum radius  $R_{\max} = 638 \mu\text{m}$  and stand-off distance  $\gamma = h_0/R_{\max} = 0.4$ . The generated pressure is recorded by a fiber optic probe hydrophone (690 ONDA, 150 MHz bandwidth) positioned off-centre at a distance of  $d_i = 950 \mu\text{m}$  to the bubble inception site,  $\approx 80 \mu\text{m}$  above the substrate, to avoid damage to the hydrophone and distortion of the hydrophone signal.

The simulations are conducted using a fully-coupled pressure-based algorithm for interfacial flows [5], which is based on a second-order finite-volume discretisation [6]. The bubble is initialised with radius  $R_0$  and gas pressure  $p_0$  at distance  $h_0$  above the substrate, as illustrated in Fig. 1b. The ambient pressure is  $p_\infty = 10^5 \text{ Pa}$ . Air is assumed to be an ideal gas with polytropic exponent  $\kappa = 1.4$ , density  $\rho_{\text{air},0} = 1.2 \text{ kg m}^{-3}$  at  $p_\infty$ , and viscosity  $\mu_{\text{air}} = 1.82 \times 10^{-5} \text{ Pa s}$ . Water is modelled by the Noble-Abel-stiffened-gas model with the properties proposed by Le Métayer and Saurel [7] and a viscosity of  $\mu_{\text{water}} = 10^{-3} \text{ Pa s}$ . Surface tension and gravity are neglected. Following previous work [1], the computational domain is resolved with a rectilinear mesh with mesh spacing  $\Delta x = 2 \mu\text{m}$  and a gradual mesh refinement near the wall, with a minimum mesh spacing of  $\Delta x_{\min} = 50 \text{ nm}$ . The time-step is adaptively chosen to satisfy a Courant number of  $\text{Co} = \Delta t |\mathbf{u}| / \Delta x < 0.7$ .

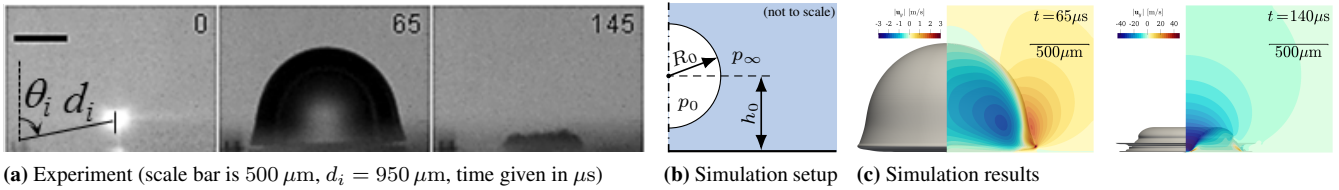
## 3 Results

Considering simulations of a bubble initially located  $h_0 = 255 \mu\text{m}$  above the substrate, the amplitude of the pressure pulse emitted at bubble inception,  $p_{i,1}$ , and the maximum bubble radius,  $R_{\max}$ , both increase for larger initial gas pressures  $p_0$  and

\* Corresponding author: e-mail fabian.denner@ovgu.de, phone +49 391 67 54912



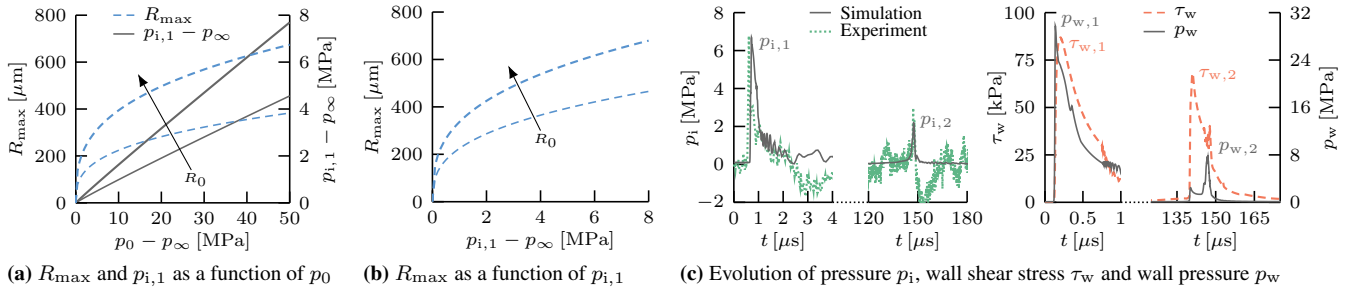
This is an open access article under the terms of the Creative Commons Attribution License, which permits use, distribution and reproduction in any medium, provided the original work is properly cited.

(a) Experiment (scale bar is  $500 \mu\text{m}$ ,  $d_i = 950 \mu\text{m}$ , time given in  $\mu\text{s}$ )

(b) Simulation setup

(c) Simulation results

**Fig. 1:** (a) High-speed images of the experiment of a laser-induced cavitation bubble with  $R_{\text{max}} = 638 \mu\text{m}$  and  $\gamma = 0.4$ . (b) Schematic of the simulation setup with the bubble near the substrate. (c) Instantaneous bubble shape and contours of the velocity perpendicular to the substrate obtained from the simulation of a bubble with  $R_{\text{max}} = 638 \mu\text{m}$  and  $\gamma = 0.4$ , initialised with  $R_0 = 80 \mu\text{m}$  and  $p_0 = 43 \text{ MPa}$ .

(a)  $R_{\text{max}}$  and  $p_{i,1}$  as a function of  $p_0$ (b)  $R_{\text{max}}$  as a function of  $p_{i,1}$ (c) Evolution of pressure  $p_i$ , wall shear stress  $\tau_w$  and wall pressure  $p_w$ 

**Fig. 2:** (a-b) Maximum radius  $R_{\text{max}}$  and first pressure peak  $p_{i,1}$  for bubbles with different initial gas pressures  $p_0$  and bubble radii  $R_0 \in \{50, 80\} \mu\text{m}$ , initially located  $h_0 = 255 \mu\text{m}$  above the substrate. (c) Evolution of the pressure signal  $p_i$ , the wall shear stress  $\tau_w$  and the wall pressure  $p_w$  for the bubble with  $R_{\text{max}} = 638 \mu\text{m}$  and  $\gamma = 0.4$ , initialised with  $R_0 = 80 \mu\text{m}$  and  $p_0 = 43 \text{ MPa}$ . The pressure signal  $p_i$  measured in the experiment of the bubble with  $R_{\text{max}} = 638 \mu\text{m}$  and  $\gamma = 0.4$ , shown in Fig. 1a, is given as a reference.

larger initial bubble radii  $R_0$ , see Fig. 2a, with  $R_{\text{max}} \propto (p_0 - p_\infty)^{1/3}$  and  $p_{i,1} \propto (p_0 - p_\infty)^{0.96} + p_\infty$ . This suggests a unique combination of reference values  $(p_{i,1}, R_{\text{max}})$ , see Fig. 2b, to select the initial conditions  $(p_0, R_0)$  of the simulation.

The simulation of the bubble initialised with  $R_0 = 80 \mu\text{m}$  and  $p_0 = 43 \text{ MPa}$ , shown in Fig. 1c, is in very good agreement with the experimental measurements, regarding the maximum bubble radius,  $R_{\text{max}} = 638 \mu\text{m}$ , and the amplitude of the pressure pulse emitted at bubble inception,  $p_{i,1} = 6.67 \text{ MPa}$ , see Fig. 2c. The amplitude of the pressure pulse emitted during bubble collapse,  $p_{i,2}$ , predicted by the simulation is also in very good agreement with the experimental measurements, considering the tolerance of the hydrophone measurements is approximately  $0.5 \text{ MPa}$ . The peak shear stress,  $\tau_{w,2} = 68.3 \text{ kPa}$ , and the peak pressure amplitude,  $p_{w,2} = 7.64 \text{ MPa}$ , associated with the collapse of the bubble, which are also shown in Fig. 2c, are similar to the values found in previous numerical studies [1, 3]. While the peak shear stress,  $\tau_{w,2}$ , is a consequence of the fast liquid jet developed during the bubble collapse, see Fig. 1c, impinging on the substrate, the peak pressure amplitude,  $p_{w,2}$ , is the result of the shock wave emitted by the bubble when it reaches its minimum volume.

## 4 Conclusions

Conducting a direct comparison of experimental measurements and numerical simulations, we introduced a unique combination of reference values  $(p_{i,1}, R_{\text{max}})$  to select the initial conditions  $(p_0, R_0)$  of the simulations. Selecting the initial conditions  $(p_0, R_0)$  to match both reference values  $(p_{i,1}, R_{\text{max}})$  measured in the experiment reproduces the dynamic behaviour of the collapsing bubble accurately and provides reliable predictions of the shear stress and pressure generated at the substrate, which we find to be in line with previous numerical studies [1, 3] for the considered representative bubble.

**Acknowledgements** This research was funded by the Deutsche Forschungsgemeinschaft (DFG, German Research Foundation), grant numbers 420239128 and 428644013.

Open access funding enabled and organized by Projekt DEAL.

## References

- [1] Q. Zeng, S. R. Gonzalez-Avila, R. Dijkink, P. Koukouvinis, M. Gavaises, and C.-D. Ohl, *J. Fluid Mech.* **846**, 341-355 (2018).
- [2] R. Dijkink and C.-D. Ohl, *Appl. Phys. Lett.* **93**, 254107 (2008).
- [3] C. Lechner, M. Koch, W. Lauterborn, and R. Mettin, *J. Acoust. Soc. Am.* **142**, 3649 (2017).
- [4] S. R. Gonzalez-Avila and C.-D. Ohl, *J. Fluid Mech.* **805**, 551-576 (2016).
- [5] F. Denner, C.-N. Xiao, B. van Wachem, *J. Comput. Phys.* **367**, 192-234 (2018).
- [6] F. Denner, F. Evrard, B. van Wachem, *J. Comput. Phys.* **409**, 109348 (2020).
- [7] O. Le Métayer and R. Saurel, *Phys. Fluids* **28**, 046102 (2016).